This is the peer reviewed author accepted manuscript (post print) version of a published work that appeared in final form in:

Jiang, Zhirui, Derrick-Roberts, Ainslie LK, Jackson, Matilda R, Rossouw, Charné, Pyragius, Carmen E, Xian, Cory, Fletcher, Janice, Byers, Sharon 2018 'Delayed development of ossification centers in the tibia of prenatal and early postnatal MPS VII mice', *Molecular genetics and metabolism*, vol. 124, no. 2, pp. 135-142

This output may not exactly replicate the final published authoritative version for which the publisher owns copyright. It is not the copy of record. This output may be used for non-commercial purposes. This version is licensed under a Creative Commons CC-BY-NC-ND 4.0 license (http://creativecommons.org/licenses/by-nc-nd/4.0/).

The final definitive published version (version of record) is available at:
https://doi.org/10.1016/j.ymgme.2018.04.014

Persistent link to the UniSA Research Outputs Repository:
http://hdl.handle.net/2440/114130

General Rights
Copyright and moral rights for the publications made accessible in the UniSA Research Outputs Repository are retained by the authors and/or other copyright owners and it is a condition of accessing publications that users recognize and abide by the legal requirements associated with these rights.

- Users may download and print one copy for the purpose of private study or research.
- You may not further distribute the material or use it for any profit-making activity or commercial gain
- You may freely distribute the persistent link identifying the publication in the UniSA Research Outputs Repository

If you believe that this document breaches copyright, please contact us and provide details. We will remove access to the work immediately and investigate your claim.

Delayed development of ossification centers in the tibia of prenatal and early postnatal MPS VII mice

Zhirui Jiang[1,2], Ainslie Derrick-Roberts[1,2,3], Matilda R Jackson[1,2], Charné Rossouw[2,3], Carmen E Pyragius[1,2], Cory J. Xian[3,4], Janice Fletcher[2], and *Sharon Byers[1,2,3]

[1] Genetics & Evolution, University of Adelaide, Adelaide, SA, Australia

[2]Genetics and Molecular Pathology, SA Pathology, Adelaide, SA, Australia

[3]Paediatrics, Adelaide Medical School, University of Adelaide, Adelaide, SA, Australia

[4]School of Pharmacy and Medical Sciences, University of South Australia, Adelaide, SA, Australia

* to whom correspondence should be addressed

Dr S Byers

Genetics and Molecular Pathology, SA Pathology (WCH site)

72 King William Rd, Nth Adelaide, SA 5006, AUSTRALIA

ph: Intl-61-8-8161-7093

email: sharon.byers@adelaide.edu.au

Abstract

Short stature is a characteristic feature of 6 types of mucopolysaccharidosis (MPS), a group of inheritable lysosomal storage disorders caused by a single enzyme deficiency. MPS patients present with progressive skeletal defects from early ages, which include short stature due to impaired cartilage-to-bone conversion (endochondral ossification). The aim of this study was to determine which murine MPS model best re-capitulates the bone length reduction phenotype of human MPS and use this model to determine the earliest development stage when disrupted endochondral ossification first appears. $GUS^{mps/mps}$ mice representing severe MPS VII displayed the greatest reduction in bone elongation and were chosen for further analysis. Tibial development was assessed from E12.5 to 6 months of age. Chondrocytes in the region of the future primary ossification center (POC) became hypertrophic at a similar age to normal in the MPS VII mouse fetus, but a delay in bone deposition was observed with an approximate 1 day delay in the formation of the POC. Likewise chondrocytes in the region of the future secondary ossification center (SOC) became hypertrophic at the same age as normal in the MPS VII early postnatal mouse. Bone deposition in the SOC was delayed by 2 days in the MPS VII proximal tibia (observed at postnatal day 14 (P14) compared to day 12 in normal). The thickness of the tibial growth plate was larger in MPS VII mice from P9 onwards. Thus, abnormal endochondral ossification therefore starts *in utero* in MPS VII and worsens with age. It is characterized by a normal timeframe for chondrocyte hypertrophy but a delay in the subsequent deposition of bone in both the primary and secondary ossification centers, accompanied by an increase in growth plate thickness. This suggests that the signals for vascular invasion and bone deposition, some of which are derived from hypertrophic chondrocytes, are altered in MPS VII.

Keywords: mucopolysaccharidosis, short stature, murine models, endochondral ossification, primary ossification center, secondary ossification center, and growth plate

1. Introduction

MPS are a group of inheritable lysosomal storage disorders resulting from the absence of, or a deficiency in, enzymes that are involved in the step-wise degradation of glycosaminoglycans (GAGs) [1]. Undegraded GAGs accumulate in multiple tissues and organs, causing a range of symptoms including hepatosplenomegaly, corneal clouding, upper airway disease, cardiac defects, progressive central nerve system deterioration and a skeletal dysplasia characterised by distinctive radiographic changes, reduced joint mobility and a short stature [1]. A skeletal disease is a common clinical manifestation in 6 types of MPS (MPS I, II, IVA, IVB, VI and VII). Bone growth velocity declines significantly after 1 year of age, with minimal long bone growth from 2 years of age, while other skeletal symptoms become progressively worse with age [1, 2]. The final height z-score of affected children ranges from -3.0 to -6.0 standard deviations below normal [3, 4]. Although hematopoietic stem cell transplantation (HSCT) and enzyme replacement therapy (ERT) are clinically approved therapies for MPS patients, only a small increase in growth velocity is observed in some MPS I, II and VI patients post HSCT or as a result of ERT [4-12], and these treatments have limited effect on the short stature [12-22].

The majority of bones in the human skeleton are formed by the process of endochondral ossification (EO) in which a cartilage template is replaced by bone. *In utero*, mesenchymal cells condense and differentiate into chondrocytes, forming a cartilaginous model of the future skeleton [23-25]. Chondrocytes in the center of the model proliferate and increase in size, while the surrounding matrix is calcified. Blood vessels invade the calcified region bringing osteogenic cells that deposit bone thus creating the POC [26]. At either end of the POC chondrocytes assemble into the characteristic zonal morphology of the growth plate. The secondary ossification centers (SOC) develop in the epiphyseal regions in a similar manner as the POC and the growth plate occupies the region between the primary and secondary ossification centers. Chondrocytes in the healthy growth plate are arranged into three morphologically distinct zones: the resting zone (RZ), proliferating zone (PZ) and hypertrophic zone

(HZ) [23, 27]. Chondrocytes enter and progress through the cell cycle to undergo several rounds of proliferation, and then withdraw from the cell cycle, progressing to hypertrophic differentiation, in order to produce a mineralised cartilage matrix that becomes new bone [28, 29].

The mechanism linking progressive cellular gag storage to skeletal pathology is not fully understood in MPS, limiting the development of effective therapies. In common with MPS patients, numerous animal models of MPS also display skeletal abnormalities [12, 30-49]. Disorganized growth plate structures have been reported in MPS VII mice [33, 36], suggesting impaired endochondral ossification. Storage of undegraded gag occurs early in life and is observed in fetal tissues from MPS VII humans, MPS VII mice and MPS VI cats [50-53]. Although the patterns of chondrogenesis, osteogenesis and ossification during limb development have been well studied in normal mice [54, 55], no comparative analyses have been reported among MPS mouse models.

In the present study, after comparing three different mouse models of MPS, the greatest reduction in bone elongation was observed in the $GUS^{mps/mps}$ strain of murine MPS VII. This strain represents the more severe end of the MPS VII phenotype spectrum. Tibial development was therefore assessed from E12.5 to 6 months of age in normal and MPS VII mice ($GUS^{mps/mps}$). It was found that, while chondrocytes underwent hypertrophic expansion and the primary and secondary ossification centers formed at the same age in both genotypes, bone deposition was delayed in both ossification centers in the MPS VII tibia. In addition, abnormal development was observed in MPS VII tibiae from as early as E15.5 and was established by birth.

2. Materials and methods

2.1 Animal husbandry

All research procedures using mice were approved by the Women's and Children's Health Network and The University of Adelaide animal ethics committees. Mice were housed on a 14/10 light/dark cycle with food and water provided *ad libitum*. Founder animals for MPS I, MPS VII (*Gus*$^{mps/mps}$ strain) and MPS VII *Gus*$^{tm(L175F)Sly}$ strain) were obtained from Jackson labs. MPS affected and normal mice were bred from heterozygous parents. Heterozygous female and male mice were paired between 3.30-4.00pm and the males removed the next morning (E0.5). Pregnant females were killed at E12.5 to E18.5 and embryos were dissected from the uterus and fixed in 10% (v/v) neutral buffered formalin (NBF). A piece of tail was collected for genotyping as previously described [12, 32, 56, 57]. Additional mice were killed between P1 and 6 months of age and the hind limbs dissected out free of soft tissue and fixed in 10% (v/v) NBF. Animal numbers can be found in supplementary Table 1.

2.2 Proximal tibia morphology

Hindlimbs were fixed in 10% (v/v) NBF for 24 hours and then decalcified in Immunocal^{TM} decalcifier (StatLab, TX, USA) for one day (up to age E18.5) or for at least seven days (P5 and older) prior to routine processing and embedding in paraffin blocks. Five microns sections were cut using a Leica RM2235 microtome (Leica Microsystems Pty Ltd, NSW, Australia). Consecutive sections were brought to water using Solv21C (United Bioscience, VIC, Australia), 100% ethanol, 70% ethanol and dH_2O and then stained for 5 min in 0.07% (w/v) Fast-Green stain (ProSciTech), dipped in 1% (v/v) acetic acid then stained with 0.07% (w/v) Safranin-O (ProSciTech) for 5 min. Sections were dehydrated in 70% ethanol, 100% ethanol then xylene. Stained samples were mounted using Leica CV Mounting Media and analyzed under an Olympus BX42 microscope (Olympus Australia Pty. Ltd., Gulfview Heights, SA, Australia) using Olympus analySIS® LS Research Olympus Soft Imaging Solutions (version 3.1) software.

2.3 Quantification analysis of area occupied by secondary ossification center

The area occupied by the secondary ossification center was measured on the proximal tibial epiphysis from normal and MPS VII mice aged from P14 days to 6m (numbers of animals analysed are shown in supplementary Table 2). Three paraffin sections per animal collected at 50μm intervals were stained with Safranin-O/Fast Green and the area occupied by the secondary ossification center measured using an Olympus BX41 microscope (Olympus Australia Pty. Ltd., Gulfview Heights, SA) and analyzed using Olympus analySIS® LS Research Olympus Soft Imaging Solutions (version 3.1) software. Measurements were averaged to yield a single value for each animal.

2.4 Statistics

Statistical significance was determined by a student's t-test using Microsoft Excel 2010. Statistical significance was assumed when $p<0.05$.

3. Results

3.1 Bone growth in mouse models of MPS

Lengths of femurs (Fig 1A), tibia (Fig 1B) and L5 vertebrae (Fig 1C) were measured on radiographs of mature 6 m old MPS I, severe MPS VII (*Gus*$^{mps/mps}$) and attenuated MPS VII (*Gus*$^{tm(L175F)Sly}$ strain) mice. Femur length was significantly decreased in all models, respectively reaching 95.5 ± 0.7 %, 66.8 ± 1.3%, and 92.6 ± 1.1% of the normal length. Tibia length was significantly reduced in the murine MPS VII severe strain (*Gus*$^{mps/mps}$) and MPS VII attenuated strain (*Gus*$^{tm(L175F)Sly}$ strain), reaching 80.9 ± 3.3 % and 96.3 ± 0.6% of normal length respectively. L5 vertebra length was reduced only in the MPS VII severe strain (*Gus*$^{mps/mps}$) reaching 85.6 ± 1.6% of the normal.

Femur growth was then measured from 14 days to 6 months of age. The growth curve followed the same pattern as normal in each case. Femur length was significantly reduced in the MPS VII severe strain (*Gus*$^{mps/mps}$) mice at all ages examined; with the differences in bone length between normal and MPS VII becoming progressively greater with age (Fig 1D), and with a growth rate (mm/day) 71.5 ± 6.3% of normal between 14 days and 1 month of age and 55.4 ± 2.7% of normal between 1 mth and 2 mths of age. Femur lengths in the MPS I (Fig 1E) and MPS VII attenuated strain (*Gus*$^{tm(L175F)Sly}$ strain) (Fig 1F) mice were not significantly different to normal at 14 day and 1 month of age, but were significantly reduced compared to normal at 3 and 6 months of age. The growth rate between 14 days and 1 month of age was 109.6 ± 6.3% and 91 ± 3.5% in MPS VII attenuated strain (*Gus*$^{tm(L175F)Sly}$ strain) and in MPS I respectively, while the growth rate between 1 month and 2 months of age was 82.6 ± 9% and 91.7 ± 3% in MPS VII attenuated strain (*Gus*$^{tm(L175F)Sly}$ strain) and in MPS I respectively. Bone lengths in murine MPS IIIA and MPS IX were the same as the normal (Supplementary Figure 1). All further analyses were performed in the severe MPS VII (*Gus*$^{mps/mps}$) mice as they displayed the greatest deviation in bone growth from the normal. The *Gus*$^{mps/mps}$ strain is hereafter referred to as MPS VII for simplicity.

3.2 Formation of the primary ossification center is slightly delayed in MPS VII tibiae

At E12.5 mesenchymal condensation was observed creating the future tibia in both normal and MPS VII (Fig 2A). Mesenchymal cells had differentiated into chondrocytes surrounded by perichondrium by E13.5 in both normal and MPS VII. At E14.5 chondrocytes in the center of the tibial model had undergone hypertrophic expansion in both genotypes, while chondrocytes on either end of this region started to flatten (Fig 2B) but had not assumed a regular columnar structure. By E15.5 capillaries had penetrated cartilage forming the marrow cavity and bone elements in 10/13 (77%) of normal tibia. In these same bones perichondrium had transformed to periosteum forming the periosteal bone collar. In contrast, in only 4/12 (33%) of MPS VII tibiae was the marrow cavity and periosteal bone collar observed and no bone elements were observed within the primary ossification center of these tibiae. At either end of the primary ossification center chondrocyte columns started to form and morphology of proliferating and hypertrophic chondrocytes was similar to normal at this stage (Fig. 2B). By E16.5 the primary ossification center was observed in both normal and MPS VII tibiae. Flattened proliferating chondrocytes and enlarged hypertrophic chondrocytes with poor columnar arrangement in MPS VII epiphysis were evident at E18.5 (Fig. 2B). While the primary ossification center continued to expand accompanied by longitudinal bone growth in both normal and MPS VII tibia during the remainder of the embryonic and early postnatal period, the MPS VII metaphysis was consistently shorter than the normal (See supplementary figure 2A and 2B for development of POC and growth plate respectively at all ages).

3.3 Formation of the secondary ossification center is delayed in MPS VII and the growth plate is thickened

Chondrocytes started to hypertrophy in the central area of the proximal tibial epiphysis at P7 (Fig 3A). Blood vessel invasion and the formation of marrow elements were observed at P10 in normal proximal tibiae followed by clear evidence of bone formation at P12. In contrast, only hypertrophic chondrocytes were observed in the MPS VII putative secondary center of ossification at P10. Blood

vessel invasion and marrow elements were observed in 1/7 MPS VII at P11, while bone elements were not observed until P14. By 2 months of age the epiphyseal region was largely occupied by trabecular bone and SOC formation was completed between 4 and 6 months of age in normal tibia. However, the area occupied by the SOC was consistently smaller in MPS VII tibia between 2 and 6 months of age (See supplementary figure 3A development of SOC at all ages).

Abnormalities were also observed in the MPS VII proximal tibial growth plate. Increased resting and hypertrophic zone length and enlarged chondrocytes were clearly observed from P9 onwards (Fig. 3B). While proliferating chondrocytes lined up in long columns in the normal control, this organisation was not as apparent in MPS VII. At postnatal two months, the epiphyseal region was largely occupied by the secondary ossification center in normal mouse tibiae, while the secondary ossification center occupied a smaller percentage of the epiphyseal area in MPS VII. Enlarged growth plate resting and hypertrophic zones were observed in MPS VII mice at all ages (See supplementary figure 3B for development of growth plate at all ages). The delayed development of the MPS VII secondary ossification center was confirmed by quantification measurement of the total epiphyseal area it occupied (Fig. 3C). Although the formation and growth of the secondary ossification center were delayed in MPS VII, the change in shape from spherical to hemispherical with age was observed in both genotypes (Fig. 3A) (See supplementary figure 3A development of SOC at all ages).

4. Discussion

Bone elongation is severely compromised in children with MPS I, II, IVA, IVB, VI and VII. Although children may fall within the normal height (length) range at birth, growth progressively slows and they fall below the 3rd percentile for height by 2-3 years of age [1, 2, 58] as GAG accumulates in skeletal tissues. GAG storage is observed in chondrocytes and osteoblasts of foetal MPS VII mice at 15 dpc and 18 dpc respectively [52]. However, it is unknown how this early storage impacts cartilage and bone development. The purpose of this study was to determine which murine model(s) best re-capitulates the reduced bone length phenotype of human MPS and to use this model to characterise tibial development from the foetus to skeletal maturity.

Initial evaluation of long bone and vertebral length at maturity revealed that the rreduction in bone length at maturity was greatest in the MPS VII (Gus$^{mps/mps}$ strain) murine model, a naturally occurring model with 0.34-1% residual enzyme activity representing severe MPS VII [31, 32, 59]. Bone length discrepancies in murine Gus$^{mps/mps}$ are consistent with human [60, 61], canine [43, 48] and feline MPS VII [62, 63]. Femur length was significantly shorter than normal from 14 days of age onwards and growth rate worsened with age. The attenuated form of MPS VII (GUS$^{tmSly(L175F)}$ strain) also displayed significantly decreased long bone, but not vertebral bone length, but the discrepancy was less than that observed in the Gus$^{mps/mps}$ strain reflecting the milder nature of this model. The murine L175F mutation is analogous to the L176F mutation which affects 20% of MPS VII patients and who display mild short stature [64, 65]. Unlike the Gus$^{mps/mps}$ strain, femur length was not significantly different to normal at younger ages in the GUS$^{tmSly(L175F)}$ strain, but as the femur growth rate decreased with age a decrease in femur length was observed at 3 and 6 months.

In contrast, bone length in the murine MPS I model was not representative of human MPS I, where MPS IH children are disproportionally short from the first year of life and attenuated cases of MPS I (MPS IH/S) have notable short trunk dwarfism [1, 66, 67]. In mature mice we found that only the

femur was significantly shorter than normal which is in agreement with Liu et al 2005 [68]. Canine and feline MPS I also do not exhibit a reduced bone length [35, 39, 43, 69]. This may be due to the higher residual enzyme activity observed in the canine and feline MPS I models, with 4% and 2.4% of normal IDUA activity respectively compared to <1% in human MPS I [70-73], which may be able to support normal bone growth. Murine MPS I has been reported to have 0-0.2% IDUA activity [43, 57], while unpublished data from our laboratory suggests that murine IDUA activity may be higher in this model (1-8% residual enzyme activity). Additional data is needed to clarify if a higher residual enzyme activity in murine MPS I results in the lack of a bone length reduction in this model.

Because of the severe failure of bone elongation in the $Gus^{mps/mps}$ MPS VII strain, it was chosen for further analyses. Early development of the MPS VII tibia was consistent with normal, with condensation of mesenchyme and formation of the cartilage anlage being complete by E13.5 and chondrocytes in the centre of the anlage undergoing hypertrophic expansion at the same time in both genotypes. The first difference in the development of the MPS VII tibia occurred with the formation of the primary ossification centre between E15.5 and E16.5. While the majority of normal tibiae (77%) displayed evidence of marrow formation and bone deposition at E15.5, only 33% of MPS VII tibiae had marrow elements present and no bone was observed at E15.5. This slight delay in development coincides with the first appearance of storage material in chondrocytes [52].

Next, we analyzed differences in the formation of the secondary ossification centre (SOC), which is the next major developmental stage in tibial growth following the formation of POC. Similar to the POC, hypertrophic expansion of chondrocytes in the centre of the epiphysis occurred at the same age in both normal and MPS VII tibiae. However, a larger time gap was observed in the formation of marrow elements and bone deposition between the genotypes than in the POC, with formation of the SOC occurring 2 days later in MPS VII. A similar delay in the deposition of bone in the SOC was observed in MPS VII dog vertebrae [12].

In this study we defined chondrocytes as hypertrophic by an increase in cell volume [74, 75]. Hypertrophic chondrocytes secrete matrix degrading enzymes including MMP9, MMP13 and ADAMTS5 [76-79]. This results in a loosening of the matrix and release of the pro-angiogenic factor VEGF from the cartilage matrix, which in turn recruits hematopoietic and osteogenic cells to form marrow and bone [29, 80-84]. Hypertrophic chondrocytes also express FGF and connective tissue growth factor (CTGF), which trigger endothelial cells for blood vessel invasion in metaphysis [85-89]. Although both normal and MPS VII chondrocytes underwent hypertrophic expansion at the same time in the POC and SOC, the subsequent delay in bone deposition suggests that MPS VII hypertrophic chondrocytes may not express one or more of these enzymes and angiogenic growth factors.

Visually the MPS VII growth plate was disorganised from E15.5 onwards and was noticeably thicker than normal from P9 onwards. Thickened growth plates are also observed in MPS VI feline and MPS I murine models [34, 47]. This is consistent with an alteration in the progression of normal phenotypic maturation as chondrocytes proliferate and hypertrophy, which is expected to negatively impact on bone elongation [90].

This study provides a detailed picture of tibial development during the latter part of pregnancy and early postnatal period in MPS VII mice. Morphologically chondrocytes in the putative primary and secondary ossification centers underwent hypertrophic expansion at the same age in normal and MPS VII mice, but bone deposition was delayed in MPS VII. This delay in bone deposition was more pronounced in the SOC than the POC and presumably coincides with a greater degree of gag storage in older chondrocytes. Together with the morphological changes observed in the growth plate these results suggest that both bone formation and elongation are affected very early in life in MPS VII.

5. Conclusions

The severe strain of murine MPS VII ($GUS^{mps/mps}$) is an ideal model for the study of bone length abnormalities as it mimics the bone length phenotype of human MPS disorders. Abnormal endochondral ossification first manifests *in utero* and worsens during postnatal long bone development in the MPS VII tibiae. While the appearance of hypertrophic chondrocytes in the POC and SOC occurs as normal, bone deposition is delayed and growth plates are thickened. This may be due to dysregulated signaling by hypertrophic chondrocytes. The results highlight the fact that bone phenotypes are established before birth in MPS VII and may explain the difficulty experienced in modulating bone growth by therapies instituted during childhood.

Acknowledgements

This project was funded by a grant from The WCH Research Foundation. AD-R was supported by Malcom Douglas Grant Research Fellowship, and CJX was supported by NHMRC Senior Research Fellowship (1042105).

Figures and Legends:

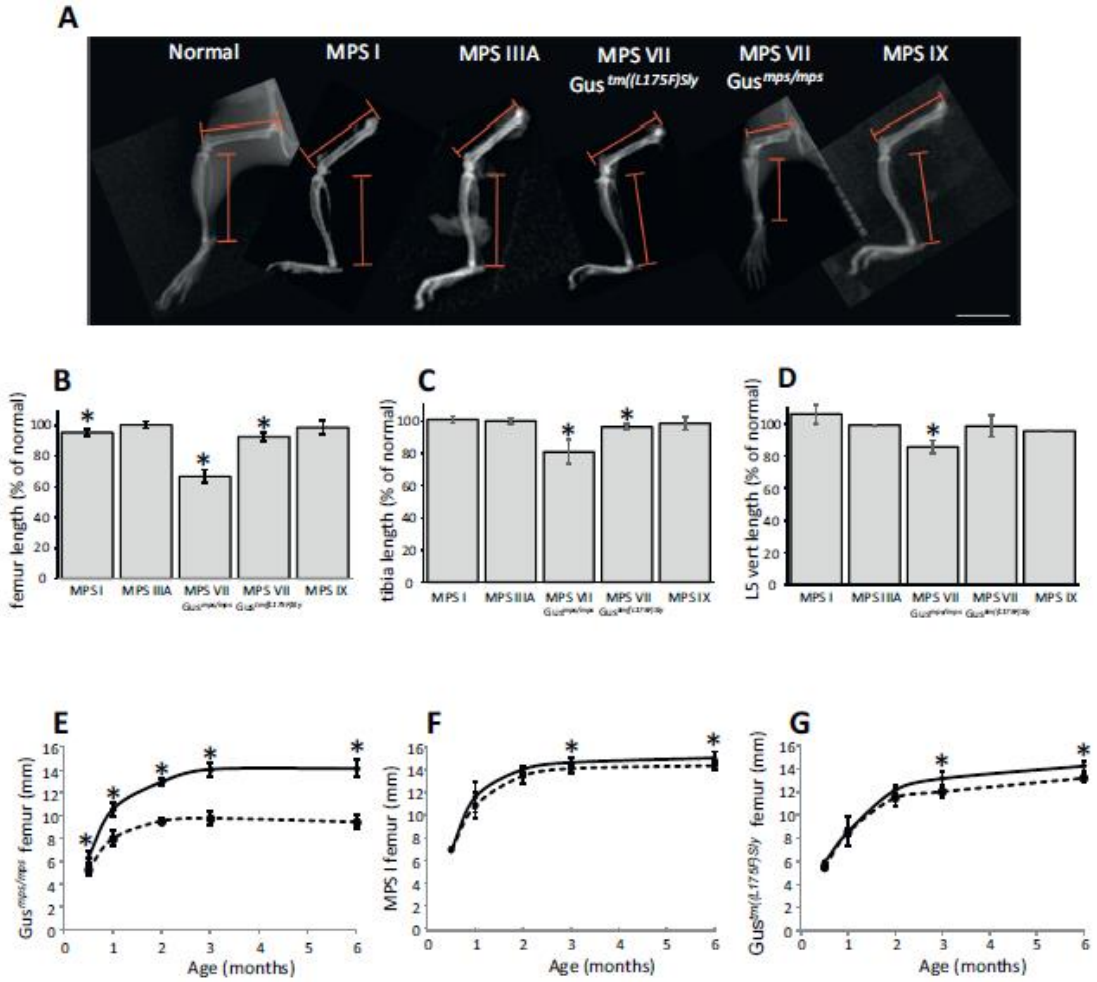


Figure 1: Bone length in murine models of MPS. Femur (A), tibia (B) and L5 vertebra (C) lengths were measured on radiographs of 6 mth old MPS I, severely affected MPS VII (*Gus*$^{mps/mps}$) and attenuated MPS VII (*Gus*$^{tm(L175F)Sly}$ strain) mice. Femur length was also measured on radiographs of severely affected MPS VII *Gus*$^{mps/mps}$ (D), attenuated MPS VII *Gus*$^{tm(L175F)Sly}$ (E) and MPS I (F) mice aged 14 days to 6 mths. Results are expressed as the % of normal littermate bone length and presented as the mean ± SEM. * denotes a significant difference ($P<0.05$) of MPS VII compared to normal.

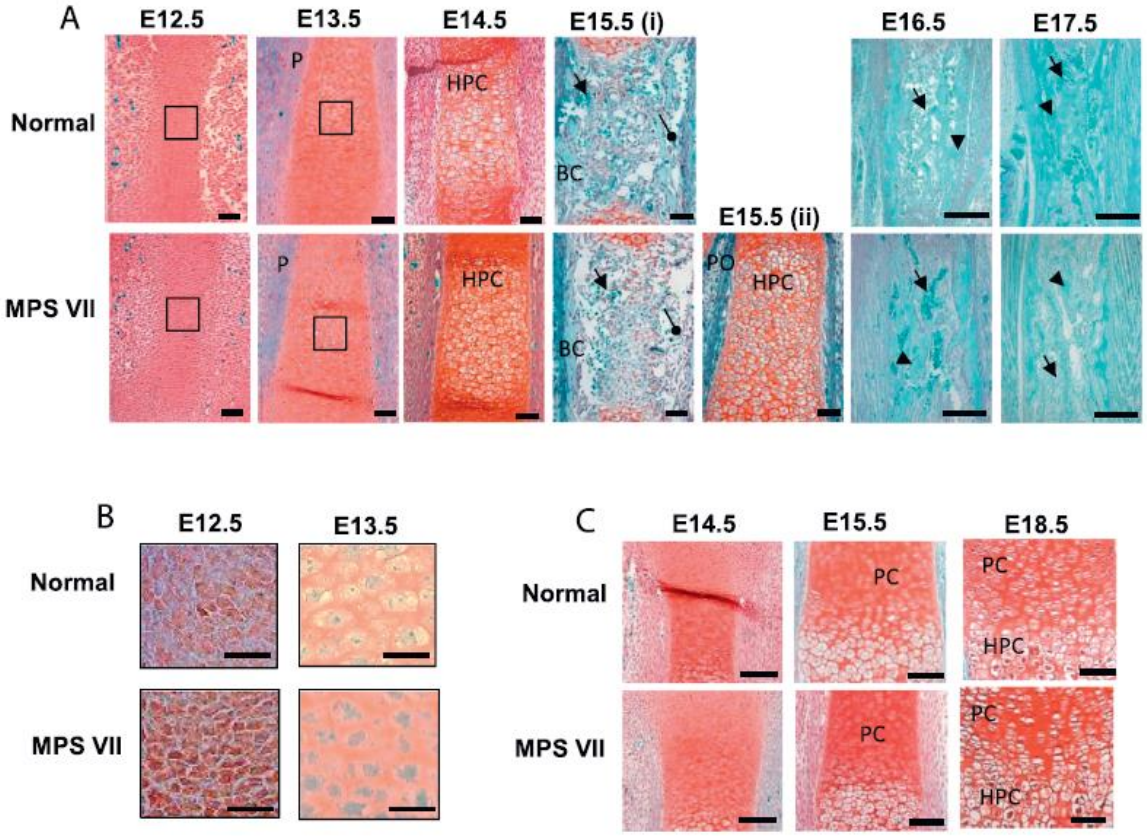


Figure 2: Formation of the primary ossification center and growth plate in the embryo. Sagittal sections of the tibial primary ossification center (A) and the adjacent proximal tibial epiphysis (B) were stained with Safranin O/fast green. Scale bar=100μm.

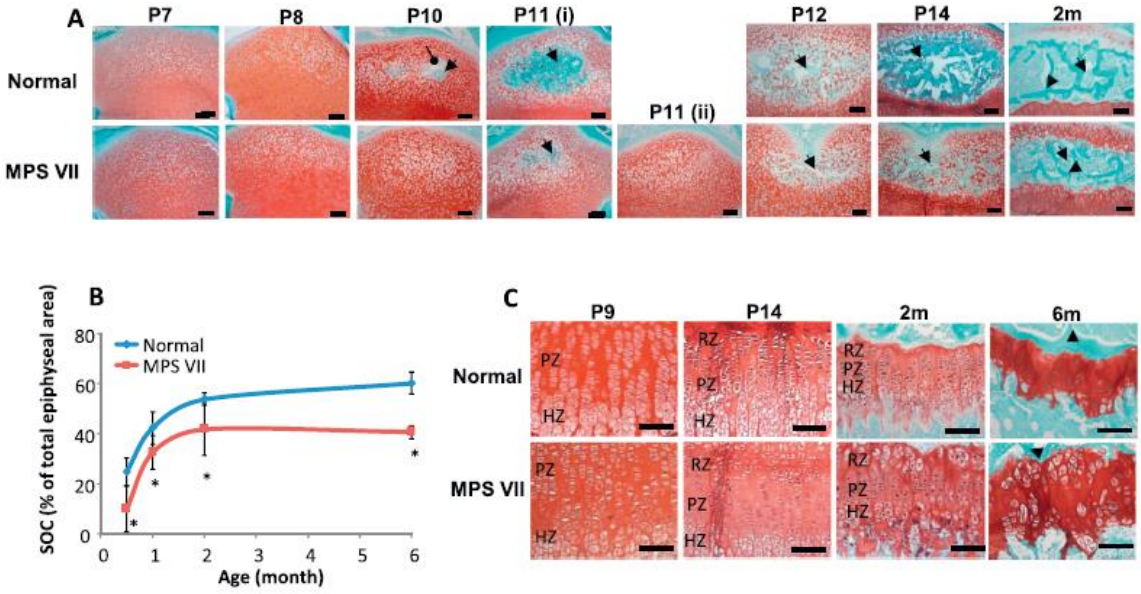


Figure 3: Formation of the secondary ossification center and expansion of the growth plate in the postnatal tibia. Sagittal sections of the proximal tibial were stained with Safranin O/fast green, showing the formation of the secondary ossification center (A) and maturation of the growth plate

(B). Scale bar=100μm. Quantitative analysis of the area of the proximal tibial epiphysis occupied by secondary ossification center (C). Results represent the mean ± SEM. * denotes a significant difference ($P<0.05$) of MPS VII compared to normal.

References.

1. Neufeld, E. and J. Muenzer, *The Mucopolysaccharidoses*, in *The metabolic and molecular bases of inherited disease*, C. Sciver, et al., Editors. 2001, McGraw hill: New York. p. 3421-3452.
2. Montaño, A.M., et al., *Growth charts for patients affected with Morquio A disease.* American Journal of Medical Genetics Part A, 2008. **146A**(10): p. 1286-1295.
3. Gardner, C.J., et al., *Growth, final height and endocrine sequelae in a UK population of patients with Hurler syndrome (MPS1H).* J Inherit Metab Dis, 2011. **34**(2): p. 489-97.
4. Polgreen, L.E., et al., *Growth and endocrine function in patients with Hurler syndrome after hematopoietic stem cell transplantation.* Bone Marrow Transplant, 2008. **41**(12): p. 1005-11.
5. Vellodi, A., et al., *Bone marrow transplantation for mucopolysaccharidosis type I: experience of two British centres.* Arch Dis Child, 1997. **76**(2): p. 92-9.
6. Kakkis, E.D., et al., *Enzyme-replacement therapy in mucopolysaccharidosis I.* N Engl J Med, 2001. **344**(3): p. 182-8.
7. Sifuentes, M., et al., *A follow-up study of MPS I patients treated with laronidase enzyme replacement therapy for 6 years.* Mol Genet Metab, 2007. **90**(2): p. 171-80.
8. Jones, S.A., et al., *The effect of idursulfase on growth in patients with Hunter syndrome: data from the Hunter Outcome Survey (HOS).* Mol Genet Metab, 2013. **109**(1): p. 41-8.
9. Pineda, M., et al., *Clinical Evolution After Enzyme Replacement Therapy in Twins with the Severe Form of Maroteaux-Lamy Syndrome.* JIMD Rep, 2016. **30**: p. 7-14.
10. Decker, C., et al., *Enzyme replacement therapy for mucopolysaccharidosis VI: Growth and pubertal development in patients treated with recombinant human N-acetylgalactosamine 4-sulfatase.* J Pediatr Rehabil Med, 2010. **3**(2): p. 89-100.
11. Schulze-Frenking, G., et al., *Effects of enzyme replacement therapy on growth in patients with mucopolysaccharidosis type II.* J Inherit Metab Dis, 2011. **34**(1): p. 203-8.
12. Peck, S.H., et al., *Delayed hypertrophic differentiation of epiphyseal chondrocytes contributes to failed secondary ossification in mucopolysaccharidosis VII dogs.* Molecular Genetics and Metabolism, 2015. **116**(3): p. 195-203.
13. Chinen, Y., et al., *Long-term therapeutic efficacy of allogenic bone marrow transplantation in a patient with mucopolysaccharidosis IVA.* Mol Genet Metab Rep, 2014. **1**: p. 31-41.
14. Herskhovitz, E., et al., *Bone marrow transplantation for Maroteaux-Lamy syndrome (MPS VI): long-term follow-up.* J Inherit Metab Dis, 1999. **22**(1): p. 50-62.
15. Tylki-Szymanska, A., et al., *Anthropometric data of 14 patients with mucopolysaccharidosis I: retrospective analysis and efficacy of recombinant human alpha-L-iduronidase (laronidase).* Mol Genet Metab, 2010. **99**(1): p. 10-7.
16. Arora, R.S., et al., *Enzyme replacement therapy in 12 patients with MPS I-H/S with homozygous p.Leu490Pro mutation.* J Inherit Metab Dis, 2007. **30**(5): p. 821.
17. Harmatz, P., et al., *The effect of galsulfase enzyme replacement therapy on the growth of patients with mucopolysaccharidosis VI (Maroteaux-Lamy syndrome).* Mol Genet Metab, 2017. **122**(1-2): p. 107-112.
18. Furujo, M., M. Kosuga, and T. Okuyama, *Enzyme replacement therapy attenuates disease progression in two Japanese siblings with mucopolysaccharidosis type VI: 10-Year follow up.* Mol Genet Metab Rep, 2017. **13**: p. 69-75.
19. Horovitz, D.D., et al., *Enzyme replacement therapy with galsulfase in 34 children younger than five years of age with MPS VI.* Mol Genet Metab, 2013. **109**(1): p. 62-9.
20. Zuber, Z., et al., *The effect of recombinant human iduronate-2-sulfatase (Idursulfase) on growth in young patients with mucopolysaccharidosis type II.* PLoS One, 2014. **9**(1): p. e85074.
21. Fox, J.E., et al., *First human treatment with investigational rhGUS enzyme replacement therapy in an advanced stage MPS VII patient.* Mol Genet Metab, 2015. **114**(2): p. 203-8.

22. Sohn, Y.B., et al., *Enzyme replacement therapy improves joint motion and outcome of the 12-min walk test in a mucopolysaccharidosis type VI patient previously treated with bone marrow transplantation.* Am J Med Genet A, 2012. **158a**(5): p. 1158-63.
23. Abad, V., et al., *The role of the resting zone in growth plate chondrogenesis.* Endocrinology, 2002. **143**(5): p. 1851-7.
24. Long, F. and D.M. Ornitz, *Development of the endochondral skeleton.* Cold Spring Harb Perspect Biol, 2013. **5**(1): p. a008334.
25. Mackie, E.J., L. Tatarczuch, and M. Mirams, *The skeleton: a multi-functional complex organ: the growth plate chondrocyte and endochondral ossification.* J Endocrinol, 2011. **211**(2): p. 109-21.
26. Caplan, A.I., *Bone development.* Ciba Found Symp, 1988. **136**: p. 3-21.
27. Burdan, F., et al., *Morphology and physiology of the epiphyseal growth plate.* Folia Histochem Cytobiol, 2009. **47**(1): p. 5-16.
28. LuValle, P. and F. Beier, *Cell cycle control in growth plate chondrocytes.* Front Biosci, 2000. **5**: p. D493-503.
29. Gerber, H.P., et al., *VEGF couples hypertrophic cartilage remodeling, ossification and angiogenesis during endochondral bone formation.* Nat Med, 1999. **5**(6): p. 623-8.
30. Abreu, S., et al., *Growth plate pathology in feline mucopolysaccharidosis VI.* Calcif Tissue Int, 1995. **57**(3): p. 185-90.
31. Birkenmeier, E.H., et al., *Murine mucopolysaccharidosis type VII. Characterization of a mouse with beta-glucuronidase deficiency.* J Clin Invest, 1989. **83**(4): p. 1258-66.
32. Macsai, C.E., et al., *Skeletal response to lentiviral mediated gene therapy in a mouse model of MPS VII.* Mol Genet Metab, 2012. **106**(2): p. 202-13.
33. Metcalf, J.A., et al., *Mechanism of shortened bones in mucopolysaccharidosis VII.* Mol Genet Metab, 2009. **97**(3): p. 202-11.
34. Nuttall, J.D., et al., *Histomorphometric analysis of the tibial growth plate in a feline model of mucopolysaccharidosis type VI.* Calcif Tissue Int, 1999. **65**(1): p. 47-52.
35. Chiaro, J.A., et al., *Postnatal progression of bone disease in the cervical spines of mucopolysaccharidosis I dogs.* Bone, 2013. **55**(1): p. 78-83.
36. Rowan, D.J., et al., *Assessment of bone dysplasia by micro-CT and glycosaminoglycan levels in mouse models for mucopolysaccharidosis type I, IIIA, IVA, and VII.* J Inherit Metab Dis, 2013. **36**(2): p. 235-46.
37. Tomatsu, S., et al., *Development of MPS IVA mouse (Galnstm(hC79S.mC76S)slu) tolerant to human N-acetylgalactosamine-6-sulfate sulfatase.* Hum Mol Genet, 2005. **14**(22): p. 3321-35.
38. Garcia, A.R., et al., *The characterization of a murine model of mucopolysaccharidosis II (Hunter syndrome).* J Inherit Metab Dis, 2007. **30**(6): p. 924-34.
39. Haskins, M.E., et al., *The pathology of the feline model of mucopolysaccharidosis I.* Am J Pathol, 1983. **112**(1): p. 27-36.
40. Haskins, M.E., et al., *Beta-glucuronidase deficiency in a dog: a model of human mucopolysaccharidosis VII.* Pediatr Res, 1984. **18**(10): p. 980-4.
41. Evers, M., et al., *Targeted disruption of the arylsulfatase B gene results in mice resembling the phenotype of mucopolysaccharidosis VI.* Proc Natl Acad Sci U S A, 1996. **93**(16): p. 8214-9.
42. Gitzelmann, R., et al., *Feline mucopolysaccharidosis VII due to beta-glucuronidase deficiency.* Vet Pathol, 1994. **31**(4): p. 435-43.
43. Herati, R.S., et al., *Radiographic evaluation of bones and joints in mucopolysaccharidosis I and VII dogs after neonatal gene therapy.* Mol Genet Metab, 2008. **95**(3): p. 142-51.
44. Schultheiss, P.C., et al., *Mucopolysaccharidosis VII in a cat.* Vet Pathol, 2000. **37**(5): p. 502-5.
45. Wang, P., et al., *Mucopolysaccharidosis VII in a Cat Caused by 2 Adjacent Missense Mutations in the GUSB Gene.* J Vet Intern Med, 2015. **29**(4): p. 1022-8.

46. Tomatsu, S., et al., *Enzyme replacement therapy in newborn mucopolysaccharidosis IVA mice: Early treatment rescues bone lesions?* Mol Genet Metab, 2014.
47. Russell, C., et al., *Murine MPS I: insights into the pathogenesis of Hurler syndrome.* Clin Genet, 1998. **53**(5): p. 349-61.
48. Smith, L.J., et al., *Effect of neonatal gene therapy on lumbar spine disease in mucopolysaccharidosis VII dogs.* Mol Genet Metab, 2012. **107**(1-2): p. 145-52.
49. Smith, L.J., et al., *Altered lumbar spine structure, biochemistry, and biomechanical properties in a canine model of mucopolysaccharidosis type VII.* J Orthop Res, 2010. **28**(5): p. 616-22.
50. Casal, M.L. and J.H. Wolfe, *Mucopolysaccharidosis Type VII in the Developing Mouse Fetus.* Pediatr Res, 2000. **47**(6): p. 750-756.
51. Crawley, A.C., et al., *Enzyme replacement therapy from birth in a feline model of mucopolysaccharidosis type VI.* J Clin Invest, 1997. **99**(4): p. 651-62.
52. Vogler, C., et al., *Early onset of lysosomal storage disease in a murine model of mucopolysaccharidosis type VII: undegraded substrate accumulates in many tissues in the fetus and very young MPS VII mouse.* Pediatr Dev Pathol, 2005. **8**(4): p. 453-62.
53. Delbecque, K., S. Gaillez, and J.P. Schaaps, *Histopathological diagnosis of a type vii mucopolysaccharidosis after pregnancy termination.* Fetal Pediatr Pathol, 2009. **28**(1): p. 1-8.
54. Patton, J.T. and M.H. Kaufman, *The timing of ossification of the limb bones, and growth rates of various long bones of the fore and hind limbs of the prenatal and early postnatal laboratory mouse.* J Anat, 1995. **186 (Pt 1)**: p. 175-85.
55. Martin, P., *Tissue patterning in the developing mouse limb.* Int J Dev Biol, 1990. **34**(3): p. 323-36.
56. Derrick-Roberts, A.L., et al., *Lentiviral-mediated gene therapy results in sustained expression of beta-glucuronidase for up to 12 months in the gus(mps/mps) and up to 18 months in the gus(tm(L175F)Sly) mouse models of mucopolysaccharidosis type VII.* Hum Gene Ther, 2014. **25**(9): p. 798-810.
57. Clarke, L.A., et al., *Murine mucopolysaccharidosis type I: targeted disruption of the murine alpha-L-iduronidase gene.* Hum Mol Genet, 1997. **6**(4): p. 503-11.
58. Hendriksz, C.J., et al., *Review of Clinical Presentation and Diagnosis of Mucopolysaccharidosis IVA.* Molecular genetics and metabolism, 2013. **110**(0): p. 54-64.
59. Vogler, C., et al., *A murine model of mucopolysaccharidosis VII. Gross and microscopic findings in beta-glucuronidase-deficient mice.* Am J Pathol, 1990. **136**(1): p. 207-17.
60. Montano, A.M., et al., *Clinical course of sly syndrome (mucopolysaccharidosis type VII).* J Med Genet, 2016. **53**(6): p. 403-18.
61. Sly, W.S., et al., *Beta glucuronidase deficiency: report of clinical, radiologic, and biochemical features of a new mucopolysaccharidosis.* J Pediatr, 1973. **82**(2): p. 249-57.
62. Fyfe, J.C., et al., *Molecular basis of feline beta-glucuronidase deficiency: an animal model of mucopolysaccharidosis VII.* Genomics, 1999. **58**(2): p. 121-8.
63. Wang, Y., et al., *IGF-I Signaling in Osterix-Expressing Cells Regulates Secondary Ossification Center Formation, Growth Plate Maturation, and Metaphyseal Formation During Postnatal Bone Development.* J Bone Miner Res, 2015. **30**(12): p. 2239-48.
64. Tomatsu, S., et al., *Missense models [Gustm(E536A)Sly, Gustm(E536Q)Sly, and Gustm(L175F)Sly] of murine mucopolysaccharidosis type VII produced by targeted mutagenesis.* Proc Natl Acad Sci U S A, 2002. **99**(23): p. 14982-7.
65. Wu, B.M., et al., *Overexpression rescues the mutant phenotype of L176F mutation causing beta-glucuronidase deficiency mucopolysaccharidosis in two Mennonite siblings.* J Biol Chem, 1994. **269**(38): p. 23681-8.
66. Laraway, S., et al., *Outcomes of Long-Term Treatment with Laronidase in Patients with Mucopolysaccharidosis Type I.* J Pediatr, 2016. **178**: p. 219-226.e1.

67. Silveri, C.P., et al., *Hurler syndrome with special reference to histologic abnormalities of the growth plate.* Clin Orthop Relat Res, 1991(269): p. 305-11.
68. Liu, Y., et al., *Liver-directed neonatal gene therapy prevents cardiac, bone, ear, and eye disease in mucopolysaccharidosis I mice.* Mol Ther, 2005. **11**(1): p. 35-47.
69. Breider, M.A., R.M. Shull, and G. Constantopoulos, *Long-term effects of bone marrow transplantation in dogs with mucopolysaccharidosis I.* Am J Pathol, 1989. **134**(3): p. 677-92.
70. Traas, A.M., et al., *Correction of Clinical Manifestations of Canine Mucopolysaccharidosis I with Neonatal Retroviral Vector Gene Therapy.* Molecular Therapy, 2007. **15**(8): p. 1423-1431.
71. He, X., et al., *Identification and characterization of the molecular lesion causing mucopolysaccharidosis type I in cats.* Mol Genet Metab, 1999. **67**(2): p. 106-12.
72. Oussoren, E., et al., *Residual alpha-L-iduronidase activity in fibroblasts of mild to severe Mucopolysaccharidosis type I patients.* Mol Genet Metab, 2013. **109**(4): p. 377-81.
73. Bunge, S., et al., *Genotype-phenotype correlations in mucopolysaccharidosis type I using enzyme kinetics, immunoquantification and in vitro turnover studies.* Biochim Biophys Acta, 1998. **1407**(3): p. 249-56.
74. Cooper, K.L., et al., *Multiple phases of chondrocyte enlargement underlie differences in skeletal proportions.* Nature, 2013. **495**: p. 375.
75. Farnum, C.E., et al., *Volume increase in growth plate chondrocytes during hypertrophy: the contribution of organic osmolytes.* Bone, 2002. **30**(4): p. 574-81.
76. Engsig, M.T., et al., *Matrix metalloproteinase 9 and vascular endothelial growth factor are essential for osteoclast recruitment into developing long bones.* J Cell Biol, 2000. **151**(4): p. 879-89.
77. Colige, A., et al., *cDNA cloning and expression of bovine procollagen I N-proteinase: a new member of the superfamily of zinc-metalloproteinases with binding sites for cells and other matrix components.* Proc Natl Acad Sci U S A, 1997. **94**(6): p. 2374-9.
78. Hurskainen, T.L., et al., *ADAM-TS5, ADAM-TS6, and ADAM-TS7, novel members of a new family of zinc metalloproteases. General features and genomic distribution of the ADAM-TS family.* J Biol Chem, 1999. **274**(36): p. 25555-63.
79. Stanton, H., et al., *ADAMTS5 is the major aggrecanase in mouse cartilage in vivo and in vitro.* Nature, 2005. **434**(7033): p. 648-52.
80. Ortega, N., D.J. Behonick, and Z. Werb, *Matrix remodeling during endochondral ossification.* Trends Cell Biol, 2004. **14**(2): p. 86-93.
81. Vu, T.H., et al., *MMP-9/gelatinase B is a key regulator of growth plate angiogenesis and apoptosis of hypertrophic chondrocytes.* Cell, 1998. **93**(3): p. 411-22.
82. Bergers, G., et al., *Matrix metalloproteinase-9 triggers the angiogenic switch during carcinogenesis.* Nat Cell Biol, 2000. **2**(10): p. 737-44.
83. Allerstorfer, D., et al., *VEGF and its role in the early development of the long bone epiphysis.* J Anat, 2010. **216**(5): p. 611-24.
84. Maes, C., et al., *Soluble VEGF isoforms are essential for establishing epiphyseal vascularization and regulating chondrocyte development and survival.* J Clin Invest, 2004. **113**(2): p. 188-99.
85. Nishida, T., et al., *CCN family 2/connective tissue growth factor (CCN2/CTGF) regulates the expression of Vegf through Hif-1α expression in a chondrocytic cell line, HCS-2/8, under hypoxic condition.* Bone, 2009. **44**(1): p. 24-31.
86. Seghezzi, G., et al., *Fibroblast growth factor-2 (FGF-2) induces vascular endothelial growth factor (VEGF) expression in the endothelial cells of forming capillaries: an autocrine mechanism contributing to angiogenesis.* J Cell Biol, 1998. **141**(7): p. 1659-73.
87. Baron, J., et al., *Induction of growth plate cartilage ossification by basic fibroblast growth factor.* Endocrinology, 1994. **135**(6): p. 2790-3.
88. Ivkovic, S., et al., *Connective tissue growth factor coordinates chondrogenesis and angiogenesis during skeletal development.* Development, 2003. **130**(12): p. 2779-91.

89. Shimo, T., et al., *Inhibition of endogenous expression of connective tissue growth factor by its antisense oligonucleotide and antisense RNA suppresses proliferation and migration of vascular endothelial cells.* J Biochem, 1998. **124**(1): p. 130-40.
90. Mackie, E.J., et al., *Endochondral ossification: how cartilage is converted into bone in the developing skeleton.* Int J Biochem Cell Biol, 2008. **40**(1): p. 46-62.